

Article

Study on Chemical Kinetics Mechanism of Ignition Characteristics of Dimethyl Ether Blended with Small Molecular Alkanes

Kai Niu¹, Baofeng Yao^{1,*}, Yonghong Xu^{1,*} , Hongguang Zhang¹, Zhicheng Shi² and Yan Wang¹

¹ Key Laboratory of Enhanced Heat Transfer and Energy Conservation of MOE, Beijing Key Laboratory of Heat Transfer and Energy Conversion, Faculty of Environment and Life, Beijing University of Technology, Beijing 100124, China; niukai1998szh@163.com (K.N.); zhanghongguang@bjut.edu.cn (H.Z.); wy5912@263.net (Y.W.)

² School of Mechanical Engineering, Beijing Institute of Technology, Beijing 100081, China; 15933731855@163.com

* Correspondence: yaobf@bjut.edu.cn (B.Y.); xyhcomeonlx@126.com (Y.X.)

Abstract: Dimethyl ether (DME)/C1-C4 alkane mixtures are ideal fuel for homogeneous charge compression ignition (HCCI) engines. The comparison of ignition delay and multi-stage ignition for DME/C1-C4 alkane mixtures can provide theoretical guidance for expanding the load range and controlling the ignition time of DME HCCI engines. However, the interaction mechanism between DME and C1-C4 alkane under engine relevant high-pressure and low-temperature conditions remains to be revealed, especially the comprehensive comparison of the negative temperature coefficient (NTC) and multi-stage ignition characteristic. Therefore, the CHEMKIN-PRO software is used to calculate the ignition delay process of DME/C1-C4 alkane mixtures (50%/50%) at different compressed temperatures (600–2000 K), pressures (20–50 bar), and equivalence ratios (0.5–2.0) and the multi-stage ignition process of DME/C1-C4 alkane mixtures (50%/50%) over the temperature of 650 K, pressure of 20 bar, and equivalence ratio range of 0.3–0.5. The results show that the ignition delay of the mixtures exhibits a typical NTC characteristic, which is more prominent at a low equivalence ratio and pressure range. The initial temperature of DME/CH₄ mixtures of the NTC region is the highest. In the NTC region, the ignition delay DME/CH₄ mixtures are the shortest, whereas DME/C₃H₈ mixtures are the longest. At low-temperature and lean-burn conditions, DME/C1-C4 alkane mixtures exhibit a distinct three-stage ignition characteristic. The time corresponding to heat release rate and pressure peak is the shortest for DME/CH₄ mixtures, and it is the longest for DME/C₃H₈ mixtures. Kinetic analysis indicates that small molecular alkane competes with the OH radical produced in the oxidation process of DME, which inhibits the oxidation of DME and promotes the oxidation of small molecular alkane. The concentration of active radicals and the OH radical production rate of elementary reactions are the highest for DME/CH₄ mixtures, and they are the lowest for DME/C₃H₈ mixtures.

Keywords: dimethyl ether; small molecule alkane; ignition delay; multi-stage ignition; low temperature; high pressure



Citation: Niu, K.; Yao, B.; Xu, Y.; Zhang, H.; Shi, Z.; Wang, Y. Study on Chemical Kinetics Mechanism of Ignition Characteristics of Dimethyl Ether Blended with Small Molecular Alkanes. *Energies* **2022**, *15*, 4652. <https://doi.org/10.3390/en15134652>

Academic Editor: Talal Yusaf

Received: 25 May 2022

Accepted: 23 June 2022

Published: 24 June 2022

Publisher's Note: MDPI stays neutral with regard to jurisdictional claims in published maps and institutional affiliations.



Copyright: © 2022 by the authors. Licensee MDPI, Basel, Switzerland. This article is an open access article distributed under the terms and conditions of the Creative Commons Attribution (CC BY) license (<https://creativecommons.org/licenses/by/4.0/>).

1. Introduction

Under the pressure of the energy crisis and environmental pollution, it is particularly important to find higher efficiency combustion modes and promising alternative fuels for internal combustion engines [1]. Due to its high oxygen content, latent heat of evaporation, and cetane number, dimethyl ether (DME) can be used as a promising diesel alternative fuel with the chemical formula of CH₃OCH₃ [2,3]. As a representation of the new combustion mode, homogeneous charge compression ignition (HCCI) has high thermal efficiency and low NO_x and soot emissions [4,5]. However, the ignition of DME HCCI engines depends

on the chemical kinetics of fuel, and there are some problems such as its narrow operating range and it being difficult to control the ignition time [6,7]. One of the effective ways to control the ignition time of HCCI engines is to mix fuels. Blending a high-octane fuel with another high-cetane fuel [8,9] could effectively expand the load range and control the ignition time, so as to meet the requirements of stable operation of HCCI engines at different load ranges.

The ignition delay is the basic parameter that reflects the ignition process of HCCI engines [10]. Researchers [11–20] conducted a large number of studies on the ignition delay characteristic of pure DME, and they found that DME has an obvious negative temperature coefficient (NTC) characteristic under medium- and low-temperature conditions, and blending a high-octane fuel with another high-cetane fuel could expand the load range and control the ignition time. Moreover, the high-temperature ignition delay characteristic of DME/C1–C4 alkane mixtures has been relatively clear, but there are few studies on the ignition delay characteristic under engine relevant low-temperature and high-pressure conditions. Burke et al. [21] studied the ignition delay characteristic of DME/CH₄ mixtures in a rapid compression machine (RCM) and shock tube (ST) over the temperature range of 600–1600 K, pressure range of 7.09275–41.54325 bar, and equivalence ratio range of 0.3–2.0, and they concluded that the ignition delay of DME/CH₄ mixtures decreased nonlinearly with the increase of pressure and equivalence ratio, and the DME dominates the ignition process during the ignition process of the mixtures. For high-temperature conditions, Tang et al. [22] investigated the ignition delay characteristic of DME/CH₄ mixtures in an ST at temperatures from 1134 to 2105 K and pressures from 1 to 10 bar. It was found that the ignition delay of the mixtures decreased with increasing DME blending ratio. The ignition delay characteristic of DME/C₂H₆ mixtures was studied using an RCM by Shi et al. [23] at the temperature of 624–913 K and pressure of 9–35 bar. They found that the ignition delay of DME/C₂H₆ mixtures decreases nonlinearly with the increase of pressure and equivalence ratio, and that the addition of C₂H₆ reduced low-temperature chain-branching routes. Zhang et al. [24] and Lu et al. [25] also studied the ignition delay characteristic DME/C₂H₆ mixtures in an ST at high-temperature conditions. Dames et al. [26] investigated the ignition delay characteristic of DME/C₃H₈ mixtures using an RCM at the temperature of 550–2000 K, pressure of 10.1325–50.6625 bar, and equivalence ratio of 0.5–2.0. It was found that the addition of DME could promote the ignition process of propane and decrease the ignition delay of the DME/C₃H₈ mixtures. Hu et al. [27] conducted experiments on an ST to measure the ignition delay of DME/C₃H₈ mixtures for high-temperature conditions and proposed a modified chemical mechanism (Mod Mech C5), which can well predict the ignition delay of pure DME, pure C₃H₈, and their mixtures. Wu et al. [28] studied the ignition delay characteristic of DME/C₄H₁₀ mixtures on an RCM under low-temperature and high-pressure conditions. The experiment results showed that DME/C₄H₁₀ mixtures exhibit an NTC and two-stage ignition characteristic at low-temperature conditions. The addition of DME enhances the reactivity of the system and nonlinearly decreases the ignition delay of the mixtures. Jiang et al. [29–34] investigated the ignition delay characteristic of DME/C₄H₁₀ mixtures under high-temperature conditions and verified the chemical mechanism of DME and C₄H₁₀. As a consequence, the NTC characteristic and interaction mechanism of DME blended with C1–C4 alkane under engine relevant low-temperature and high-pressure conditions are unclear, and it is necessary to further investigate the ignition delay characteristic and interaction mechanism of DME/C1–C4 alkane.

Some relevant scholars [35,36] found that DME exhibits a typical three-stage ignition and heat release phenomenon at low-temperature and lean-burn conditions, which are a low temperature reaction, high temperature first stage reaction, and high temperature second stage reaction, respectively. Iijima et al. [37] conducted experiments on an HCCI engine to study the multi-stage heat release phenomenon of DME/CH₄ mixtures. Interestingly, they found that with the increase of methane blending ratio, the heat release rate (HRR) of the high temperature first stage reaction decreased, and the HRR of the high temperature

second stage reaction increased. Shimizu et al. [38] and Komatsu et al. [39] conducted experiments on an HCCI engine to investigate the multi-stage heat release phenomenon of DME/CH₄ mixtures. It was found that the formation of HCHO in the low-temperature reaction stage is determined by the concentration of DME and independent of the concentration of CH₄. Thus, the multi-stage ignition phenomenon of DME blended with C1-C4 small molecular alkane at low-temperature and lean-burn conditions is rarely studied. Meanwhile, the interaction mechanism between DME and C1-C4 alkane is still unclear and needs further analysis.

As is known based on the above literature review, DME blended with C1-C4 small molecular alkane mixtures has an obvious NTC characteristic at low-temperature conditions, but the four mixtures exhibit different NTC characteristics. The comprehensive comparison of different NTC properties of DME blended with C1-C4 alkane mixtures under engine relevant low-temperature and high-pressure conditions has not been reported, and there are few studies on the interaction mechanism between DME and C1-C4 alkane in the NTC region. In addition, DME blended with C1-C4 alkane mixtures exhibits a multi-stage ignition characteristic at low-temperature and lean-burn conditions, but the multi-stage ignition characteristic of four mixtures is different. There are few comprehensive comparative studies on the multi-stage ignition of DME blended with C1-C4 alkane. Therefore, it is necessary to investigate the ignition delay and multi-stage ignition characteristic of DME blended with C1-C4 alkane mixtures and to analyze the interaction mechanism between DME and C1-C4 alkane by chemical kinetics.

In this study, the CHEMKIN-PRO software is used to calculate the ignition delay of DME/C1-C4 alkane mixtures under engine relevant low-temperature and high-pressure conditions and to calculate the ignition delay at high-temperature conditions as a comparison. Moreover, the pressure and HRR of DME/C1-C4 alkane mixtures at low-temperature and lean-burn conditions are calculated. The multi-stage ignition and NTC characteristic of four mixtures are compared, and the interaction mechanism between DME and C1-C4 alkane is analyzed by chemical reaction kinetics. The primary objective of the current study is to investigate the comparison of C1-C4 alkane addition to DME HCCI combustion via the simulation method. Furthermore, the interaction mechanism between DME and C1-C4 alkane during high-pressure and low-temperature ignition is clarified through chemical kinetic analysis. The comparison of ignition delay and multi-stage ignition for DME/C1-C4 alkane mixtures can provide theoretical guidance for expanding the load range and controlling the ignition time of DME HCCI engines.

2. Calculation Method

Numerical simulations were conducted using CHEMKIN-PRO software. The calculation assumes a closed 0-D homogeneous batch reactor at adiabatic and constant volume conditions. Default values from CHEMKIN were used for the solver tolerances and solver time-steps. The NUIG Aramco Mech 3.0 mechanism containing detailed DME and C1-C4 chemistries was developed by Combustion Chemistry Center at NUI Galway in 2018 and can be used to simulate the ignition delay and multi-stage ignition behavior of C1-C4-based hydrocarbons over a wide variety of experimental conditions. The mechanism has been validated against the data from STs, RCMs, flow reactors, and jet-stirred reactors [40]. No modifications to reaction rates were made to the mechanisms considered in this study.

Initial conditions were selected based on relevance to existing experimental ST and RCM data and engine relevant low-temperature and high-pressure conditions, particularly the initial temperatures and pressures. The ignition delay simulations were carried out over the temperature range of 600–2000 K in 50 K increments, the pressure range of 10–50 bar in 10 bar increments, and the equivalence ratio range of 0.5–2.0 in 0.5 increments. However, the multi-stage ignition simulations were conducted at the equivalence ratio of 0.3–0.5 in 0.1 increments, the temperature of 650 K, and the pressure of 20 bar. In this study, the blending ratio of DME (X_{DME}) of 50% was kept constant for all fuels. The ignition characteristic of DME blended with small molecular alkane changed significantly under

DME blending ratio of 50% conditions. The DME blending ratio of 50% is expressed as the mole fraction of DME in fuel mixtures. The mixture compositions and initial conditions are given in Table 1.

Table 1. Mixture compositions and initial conditions for 0-D homogeneous batch reactor simulations.

| Type | Fuel | X _{DME} (%) | T _c (T) | P _c (bar) | φ (-) |
|----------------------|------------------------------------|----------------------|--------------------|----------------------|---------|
| Ignition delay | DME/CH ₄ | 50% | 600–2000 | 10–50 | 0.5–2.0 |
| | DME/C ₂ H ₆ | | | | |
| | DME/C ₃ H ₈ | | | | |
| | DME/C ₄ H ₁₀ | | | | |
| Multi-stage ignition | DME/CH ₄ | 50% | 650 | 20 | 0.3–0.5 |
| | DME/C ₂ H ₆ | | | | |
| | DME/C ₃ H ₈ | | | | |
| | DME/C ₄ H ₁₀ | | | | |

The first-stage ignition delay, τ_1 , is defined as the duration between the timing of $t = 0$, and the timing of the first peak in the temperature rising rate. The second-stage ignition delay, τ_2 , is defined as the duration from the timing at the first peak to the timing at the second peak in the temperature rising rate during ignition. The total ignition delay τ is the sum of τ_1 and τ_2 . The DME/C1-C4 alkane mixtures display two-stage ignition behavior, which are low temperature reaction (LTR) and high temperature reaction (HTR). The first-stage ignition delay τ_1 is the LTR and the second-stage ignition delay τ_2 is the transition time from the LTR to HTR. The total ignition delay τ is the HTR. The character ϕ stands for equivalence ratio. The equivalence ratio ϕ is defined as the ratio of the theoretical air quantity required for complete combustion to the actual air quantity supplied during fuel combustion. The engine relevant low-temperature and high-pressure conditions refer to the thermodynamic conditions of the engine cylinder.

3. Results and Discussion

3.1. Ignition Delay Characteristic of DME/C1-C4 Alkane Mixtures

3.1.1. Comparison of Ignition Delay Characteristic of DME/C1-C4 Alkane Mixtures at Different Equivalence Ratios

Figure 1 shows the comparison of the ignition delay of DME/C1-C4 alkane (50%/50%) mixtures at different equivalence ratios of 0.5, 1.0, 1.5, and 2.0. It can be observed that the addition of small molecular alkane to DME results in the extension of the ignition delay, namely, the addition of small molecular alkane inhibits the ignition process of DME. The mixtures present an obvious NTC characteristic in the 750–900 K temperature range as the temperature increases. In the NTC region, DME/CH₄ mixtures have the highest initial temperature, whereas DME/C₄H₁₀ mixtures have the most obvious NTC characteristic. DME/CH₄ mixtures have the shortest ignition delay and DME/C₃H₈ mixtures have the longest. DME/C₂H₆ and DME/C₄H₁₀ mixtures are between the above two mixtures, and DME/C₄H₁₀ mixtures are shorter than DME/C₂H₆ mixtures. The ignition delay shows a significant decreasing trend with the increasing equivalence ratio. This is because the increase of the equivalence ratio could increase fuel concentration, thereby speeding up the reaction rate and decreasing the ignition delay. Moreover, the stronger sensitivity of the equivalence ratio is observed in the NTC region compared to that in the low- and high-temperature region.

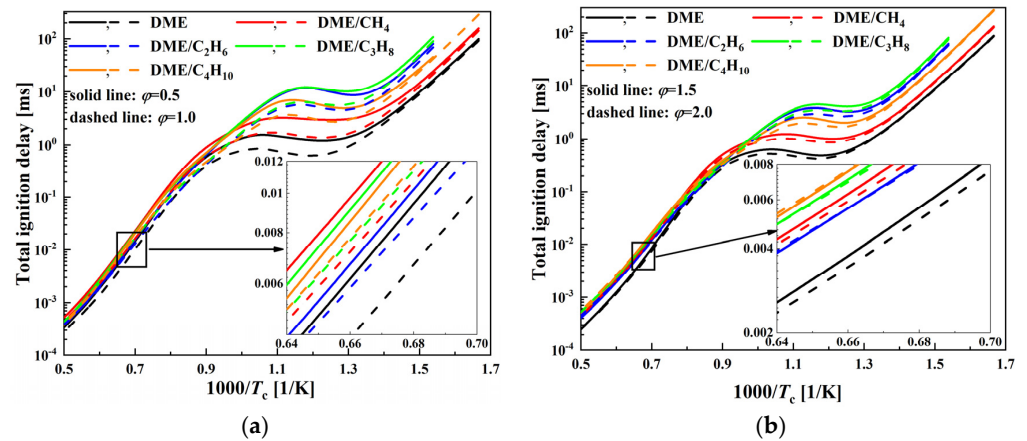


Figure 1. Comparison of ignition delay of DME/C1-C4 alkane mixtures for various equivalence ratios at $P_c = 20$ bar: (a) $\phi = 0.5, 1.0$ and (b) $\phi = 1.5, 2.0$.

The ignition delay of mixtures is further plotted as a function of equivalence ratio at different compressed temperatures, and at the pressure of 20 bar. It can be seen from Figure 2 that the ignition delay exhibits an obvious nonlinear decreasing trend with the increase of equivalence ratio, and this effect becomes significant at a lower equivalence ratio. At temperatures of 650 and 800 K, the ignition delay from long to short is for DME/C₃H₈, DME/C₂H₆, DME/C₄H₁₀, and DME/CH₄ mixtures. However, at a temperature of 1500 K, the ignition delay of DME/CH₄ mixtures is the shortest. In the NTC region, the increase of equivalence ratio has the most significant effect on the ignition delay for DME/C₃H₈ mixtures and the least effect on DME/CH₄ mixtures.

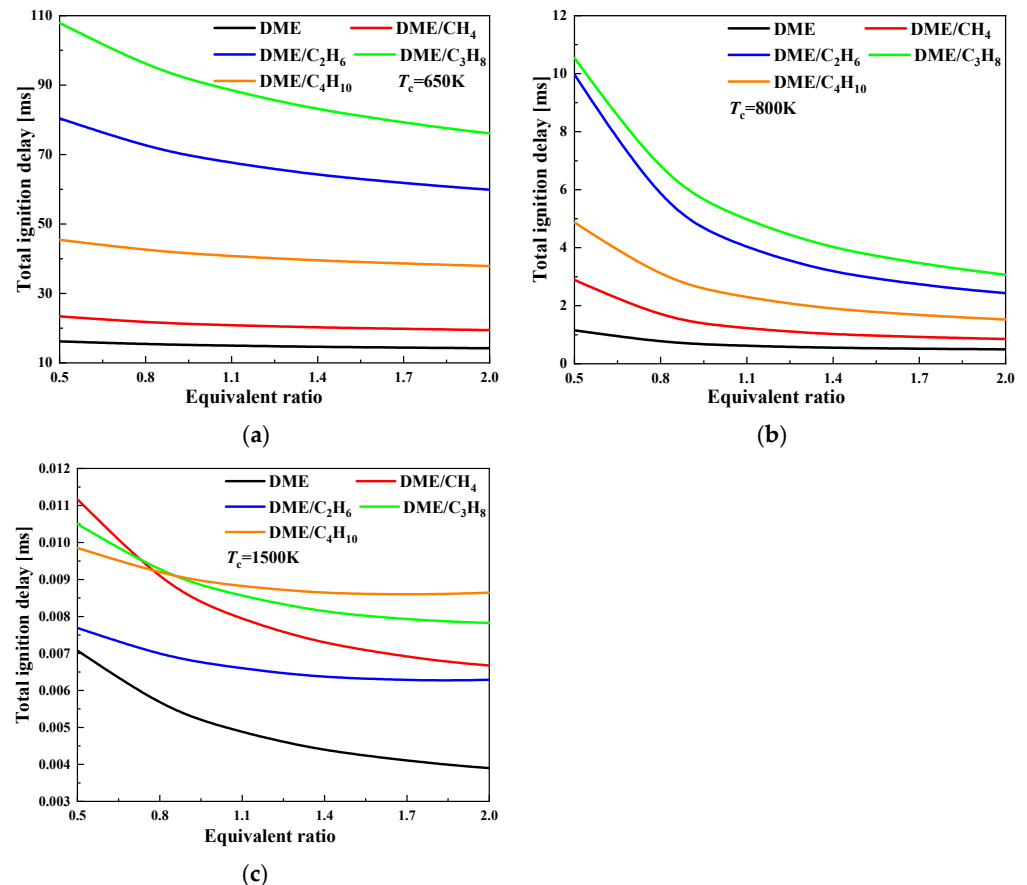


Figure 2. Ignition delay as a function of equivalence ratio for various compressed temperatures at $P_c = 20$ bar: (a) $T_c = 650$ K; (b) $T_c = 800$ K; and (c) $T_c = 1500$ K.

3.1.2. Comparison of Ignition Delay Characteristic of DME/C1-C4 Alkane Mixtures at Different Compressed Pressures

The comparison of the ignition delay of DME/C1-C4 alkane (50%/50%) mixtures is studied at compressed pressures of 20, 30, 40, and 50 bar. In Figure 3, the mixtures exhibit an obvious NTC characteristic in the 800–950 K temperature range. In the NTC region, DME/CH₄ mixtures have the shortest ignition delay and DME/C₃H₈ mixtures have the longest. DME/C₂H₆ and DME/C₄H₁₀ mixtures are between the above two mixtures, and DME/C₄H₁₀ mixtures are shorter than DME/C₂H₆ mixtures. DME/CH₄ mixtures have the highest initial temperature, whereas DME/C₄H₁₀ mixtures have the most obvious NTC characteristic. The ignition delay shows a typical decreasing trend with increasing compressed pressure, which is similar to the effect of the equivalence ratio. This is because the increase of the compressed pressure could increase mixtures' concentration and the number of effective molecular collisions, thereby speeding up the reaction rate and decreasing the ignition delay. In addition, the stronger dependence of the equivalence ratio is found in the NTC region when compared to the low- and high-temperature region.

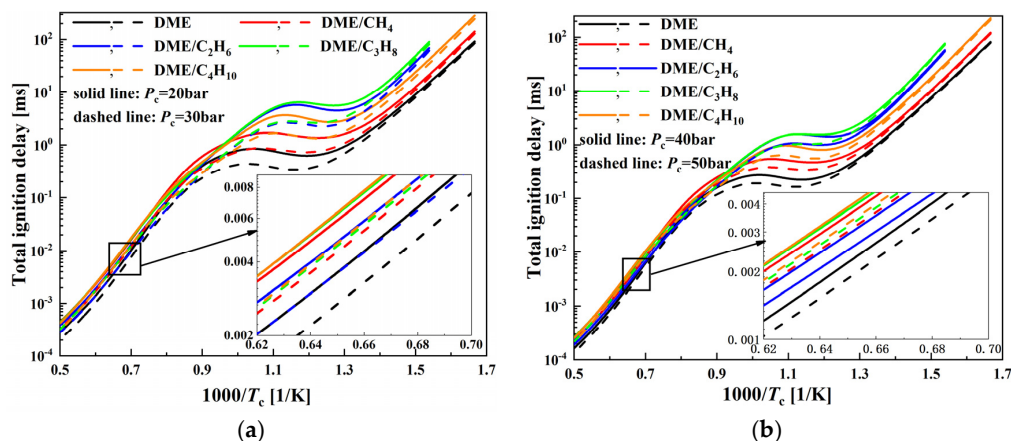


Figure 3. Comparison of ignition delay of DME/C1-C4 alkane mixtures for various compressed pressures at $\phi = 0.5$: (a) $P_c = 20, 30$ bar and (b) $P_c = 40, 50$ bar.

The ignition delay of mixtures is further plotted as a function of pressures at different compressed temperatures and at the equivalence ratio of 1.0 in Figure 4. With the increase of compressed pressure, the ignition delay decreases nonlinearly and the effect becomes obvious at lower pressure. At a temperature of 800 K, the increase of equivalence ratio has the most obvious effect on the ignition delay for DME/C₃H₈ mixtures and the least effect on DME/CH₄ mixtures, which is similar to the effect of the equivalence ratio.

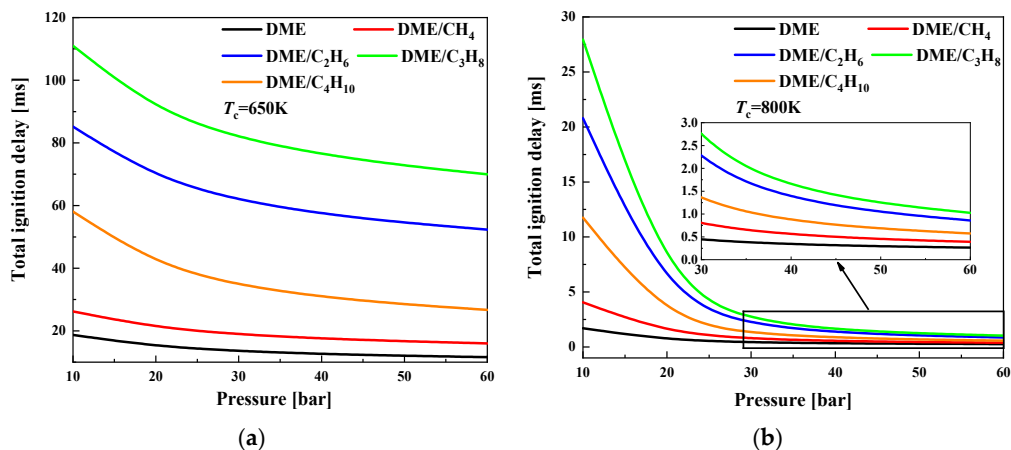


Figure 4. Cont.

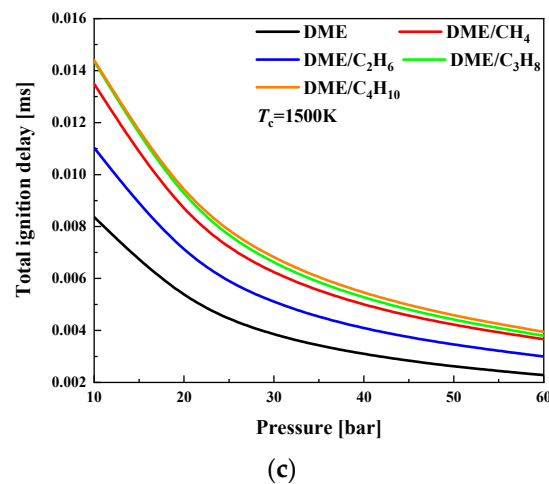


Figure 4. Ignition delay as a function of compressed pressures for various compressed temperatures at $\varphi = 0.5$: (a) $T_c = 650$ K; (b) $T_c = 800$ K; and (c) $T_c = 1500$ K.

3.1.3. Mole Fraction Analysis

To clarify the interaction mechanism between DME and C1-C4 alkane during the ignition process, the mole fraction of certain important species is performed at $P_c = 20$ bar, $\varphi = 0.5$, and $T_c = 650, 800,$ and 1500 K. Moreover, the free radicals such as H, O, OH, HO_2 , H_2O_2 , R, and RO_2 play an important role during the ignition process; thus, these free radicals are used to represent the ignition chemistry of the mixtures.

In order to better compare the mole fraction profile of DME/C1-C4 alkane mixtures, it is essential to use the log-log coordinate in Figures 5–7. Figure 5 show the mole fraction as a function of time at $P_c = 20$ bar, $\varphi = 0.5$, and $T_c = 650$ K. As presented in Figure 5, the addition of C1-C4 alkane to DME will decrease the mole fraction of H, O, OH, HO_2 , R, and RO_2 radicals and delay the time corresponding to the mole fraction peak. In the DME blended with C1-C4 alkane mixtures, the mole fraction of H, O, OH, HO_2 , R, and RO_2 radicals follows the order $\text{DME}/\text{CH}_4 > \text{DME}/\text{C}_4\text{H}_{10} > \text{DME}/\text{C}_2\text{H}_6 > \text{DME}/\text{C}_3\text{H}_8$ and the time corresponding to the mole fraction peak increases in the order $\text{DME}/\text{CH}_4 < \text{DME}/\text{C}_4\text{H}_{10} < \text{DME}/\text{C}_2\text{H}_6 < \text{DME}/\text{C}_3\text{H}_8$. Consequently, the ignition delay increases in the order $\text{DME}/\text{CH}_4 < \text{DME}/\text{C}_4\text{H}_{10} < \text{DME}/\text{C}_2\text{H}_6 < \text{DME}/\text{C}_3\text{H}_8$.

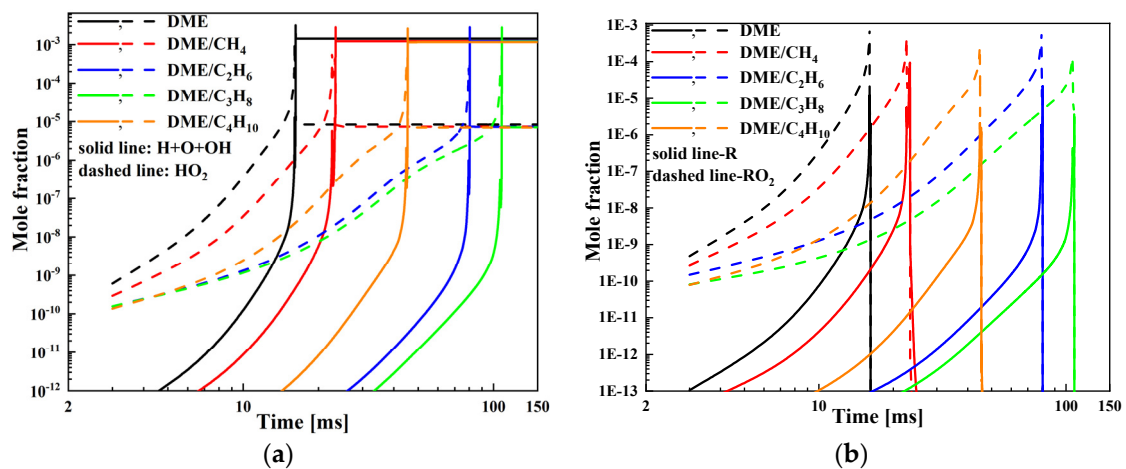


Figure 5. Mole fraction of various species for DME/C1-C4 alkane mixtures at $T_c = 650$ K, $P_c = 20$ bar, and $\varphi = 0.5$: (a) H, O, OH, HO_2 and (b) R, RO_2 .

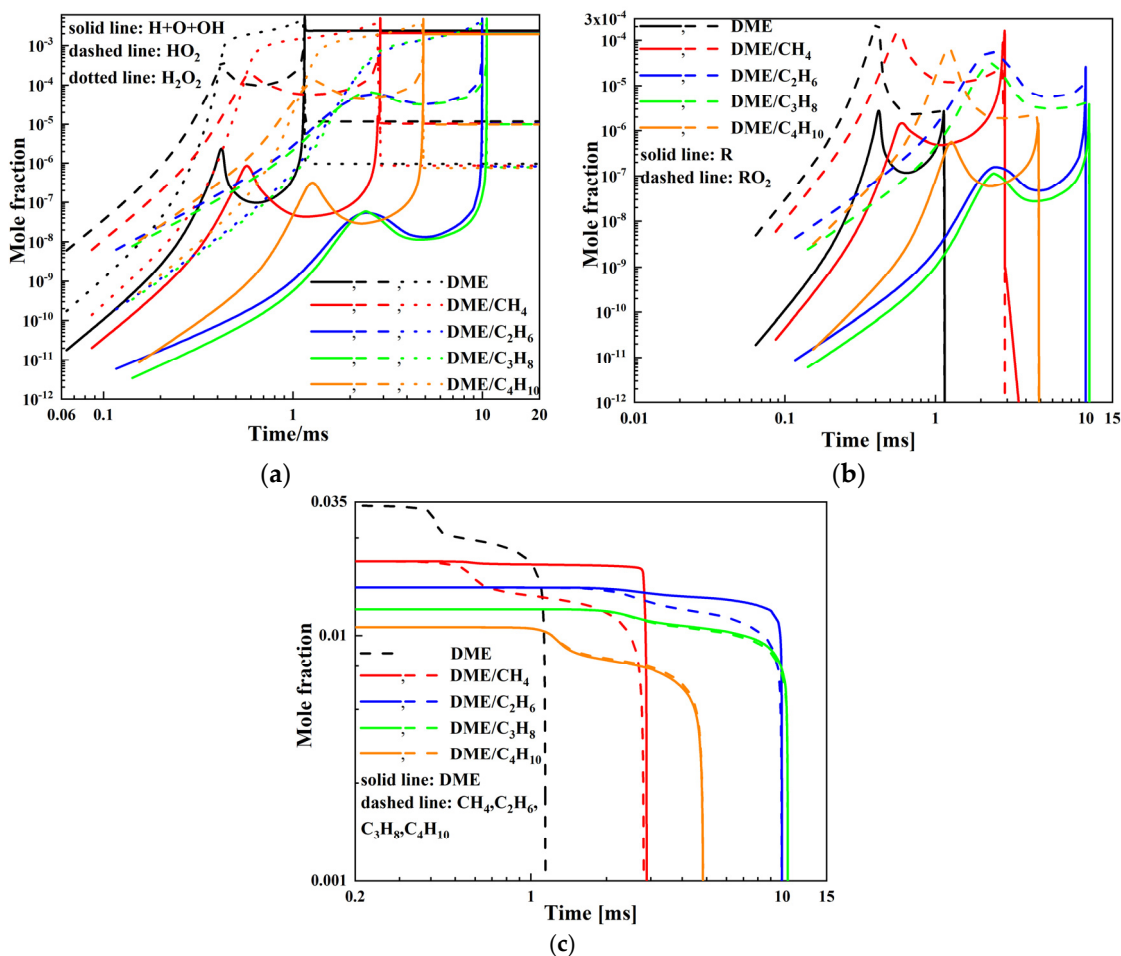


Figure 6. Mole fraction of various species for DME/C1-C4 alkane mixtures at $T_c = 800$ K, $P_c = 20$ bar, and $\phi = 0.5$: (a) H, O, OH, HO_2 , H_2O_2 ; (b) R, RO_2 ; and (c) DME, CH_4 , C_2H_6 , C_3H_8 , C_4H_{10} .

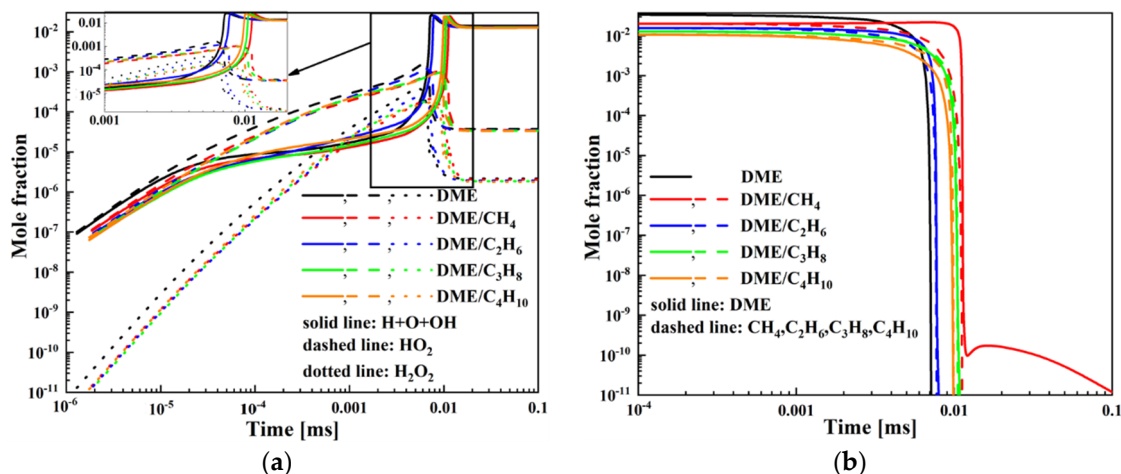


Figure 7. Mole fraction of various species for DME/C1-C4 alkane mixtures at $T_c = 1500$ K, $P_c = 20$ bar, and $\phi = 0.5$: (a) H, O, OH, HO_2 , H_2O_2 and (b) DME, CH_4 , C_2H_6 , C_3H_8 , C_4H_{10} .

The mole fraction as a function of time at $P_c = 20$ bar, $\phi = 0.5$, and $T_c = 800$ K is presented in Figure 6. As presented in Figure 6a,b, the addition of C1-C4 alkane to DME will decrease the mole fraction of H, O, OH, HO_2 , H_2O_2 , R, and RO_2 radicals and delay the time corresponding to the mole fraction peak. DME/ CH_4 mixtures have the highest mole fraction of H, O, OH, HO_2 , H_2O_2 , R, and RO_2 radicals, and DME/ C_3H_8 mixtures

have the lowest. DME/C₂H₆ and DME/C₄H₁₀ mixtures are between the above two mixtures, and DME/C₄H₁₀ mixtures are higher than DME/C₂H₆ mixtures. The time corresponding to the mole fraction peak increases in the order DME/CH₄ < DME/C₄H₁₀ < DME/C₂H₆ < DME/C₃H₈. It can be observed in Figure 6c that DME, C₃H₈, and C₄H₁₀ present distinct two-stage ignition behavior, whereas CH₄ and C₂H₆ exhibit obvious single-stage ignition behavior. Both DME and C1-C4 alkane are dominantly consumed by H-abstraction reactions with OH radicals at low temperatures. C1-C4 alkane compete with the OH radicals produced in the oxidation process of DME, which inhibits the oxidation of DME and promotes the oxidation of C1-C4 alkane. The first stage ignition is mainly dominated by DME during the ignition process of DME/CH₄ and DME/C₂H₆ mixtures, and the first stage ignition is mainly dominated by DME, propane, and n-butane during the ignition process of DME/C₃H₈ and DME/C₄H₁₀ mixtures. The heat and free radicals produced during the first-stage ignition determine the second-stage ignition when the mixtures display two-stage ignition behavior. The time corresponding to the complete consumption of DME or C1-C4 alkane increases in the order DME/CH₄ < DME/C₄H₁₀ < DME/C₂H₆ < DME/C₃H₈. Consequently, the ignition delay of DME/CH₄ mixtures is the shortest and DME/C₃H₈ mixtures is the longest. DME/C₂H₆ and DME/C₄H₁₀ mixtures are between the above two mixtures, and DME/C₂H₆ mixtures are longer than DME/C₄H₁₀ mixtures.

The mole fraction as a function of time at $P_c = 20$ bar, $\varphi = 0.5$, and $T_c = 1500$ K is presented in Figure 7. As presented in Figure 7a, the addition of C1-C4 alkane to DME will decrease the mole fraction of H, O, OH, HO₂, and H₂O₂ radicals and delay the time corresponding to the mole fraction peak. In the four mixtures of DME blended with C1-C4 alkane, the mole fraction of H, O, OH, HO₂, and H₂O₂ radicals follows the order DME/C₂H₆ > DME/C₄H₁₀ > DME/C₃H₈ > DME/CH₄ and the time corresponding to the mole fraction peak increases in the order DME/C₂H₆ < DME/C₄H₁₀ < DME/C₃H₈ < DME/CH₄. It can be seen from Figure 7b that DME, CH₄, C₂H₆, C₃H₈, and C₄H₁₀ all display distinct single-stage ignition behavior during the high-temperature ignition. The time corresponding to C1-C4 alkane consumption increases in the order DME/C₂H₆ < DME/C₄H₁₀ < DME/C₃H₈ < DME/CH₄. Consequently, the ignition delay increases in the order DME/C₂H₆ < DME/C₄H₁₀ < DME/C₃H₈ < DME/CH₄.

3.1.4. Sensitivity Analysis

To further investigate the effect of small molecular alkane on DME, sensitivity analysis on the ignition delay of DME/C1-C4 alkane mixtures was carried out at the temperature of 800 and 1500 K, the pressure of 20 bar, and equivalence ratio of 0.5. The reactions of the positive coefficient inhibit the ignition, whereas the negative coefficient promotes the ignition. The sensitivity coefficient (S) is defined as

$$S = \frac{\tau(2.0k_i) - \tau(k_i)}{\tau(k_i)} \quad (1)$$

where τ is the ignition delay and k_i is the pre-exponential factor of the i th reaction.

The sensitivity coefficient of the ignition delay for mixtures at the temperature of 800 and 1500 K is shown in Figure 8. At the temperature of 800 K, the most promoting reaction is R431 $\text{CH}_3\text{OCH}_3 + \text{OH} \rightleftharpoons \text{CH}_3\text{OCH}_2 + \text{H}_2\text{O}$, and R453 $\text{CH}_2\text{OCH}_2\text{O}_2\text{H} \rightleftharpoons 2\text{CH}_2\text{O} + \text{OH}$ is the important inhibiting reaction. The sensitivity coefficient of R453 is larger than the sensitivity coefficient of R431, which indicates that the ignition chemistry is in the NTC region. Moreover, R199 $\text{C}_2\text{H}_6 + \text{OH} \rightleftharpoons \text{C}_2\text{H}_5 + \text{H}_2\text{O}$, R510 $\text{C}_3\text{H}_8 + \text{OH} \rightleftharpoons \text{NC}_3\text{H}_7 + \text{H}_2\text{O}$, and R1112 $\text{C}_4\text{H}_{10} + \text{OH} \rightleftharpoons \text{PC}_4\text{H}_9 + \text{H}_2\text{O}$ are dominant inhibiting reactions for DME/C₂H₆, DME/C₃H₈, and DME/C₄H₁₀ mixtures. The reactions R45, R199, R510, and R1112 compete with reaction R431 for OH radicals and inhibit the oxidation process of DME. As shown in Figure 8b, at the temperature of 1500 K, the most promoting and inhibiting reactions are R5 $\text{O}_2 + \text{H} \rightleftharpoons \text{O} + \text{OH}$ and R48 $\text{CH}_3 + \text{HO}_2 \rightleftharpoons \text{CH}_4 + \text{O}_2$, respectively. In addition, the sensitivity coefficient of R5 or R48 increases in the order

$DME/C_2H_6 < DME/C_4H_{10} < DME/C_3H_8 < DME/CH_4$. Therefore, the ignition delay increases in the order $DME/C_2H_6 < DME/C_4H_{10} < DME/C_3H_8 < DME/CH_4$.

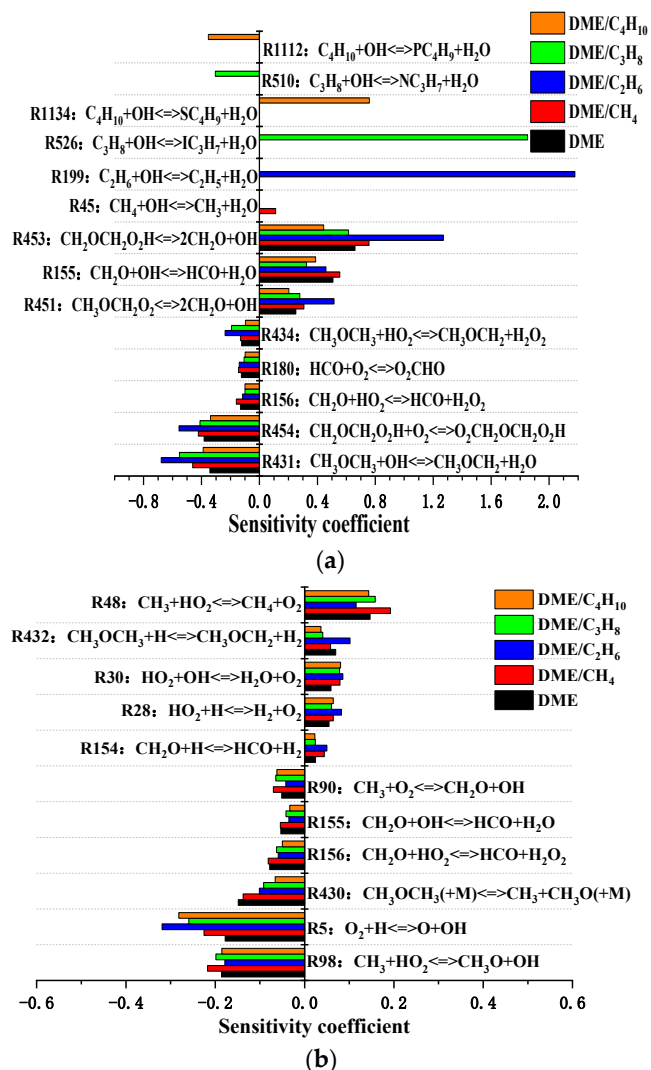


Figure 8. Sensitivity of the ignition delay of DME/C1-C4 alkane mixtures for various compressed temperatures at $P_c = 20$ bar and $\varphi = 0.5$: (a) $T_c = 800$ K and (b) $T_c = 1500$ K.

3.1.5. Production Rate Analysis

The production rate of OH radicals of the important elementary reactions for mixtures is investigated at $T_c = 650, 800,$ and 1500 K in Figure 9. The important elementary reactions including OH radicals are listed in Table 2. As seen in Figure 9a,b, at $T_c = 650$ and 800 K, the sum of the reactions R450, R451, and R453 or the sum of reactions R456 and R462 of the OH radicals production rate for pure DME is the highest, and the time corresponding to the production rate peak is the earliest. In the four mixtures of DME blended with small molecular C1-C4 alkane, for the production rate of OH radicals of reactions, the sum of R450, R451, and R453 or the sum of R456 and R462 follows the order $DME/CH_4 > DME/C_4H_{10} > DME/C_2H_6 > DME/C_3H_8$ and the time corresponding to the production rate peak increases in the order $DME/CH_4 < DME/C_4H_{10} < DME/C_2H_6 < DME/C_3H_8$. In addition, the production rate of OH radicals of the sum of R450, R451, and R453 is larger than the OH radicals production rate of the sum of R456 and R462, which indicates that the ignition chemistry is in the NTC region for DME/C1-C4 alkane mixtures. The reactions R155, R431, R45, R199, R510, R526, R1112, and R1134 are the CH_2O , DME, CH_4 , C_2H_6 , C_3H_8 , and C_4H_{10} consuming OH radicals, respectively. The production rate of OH radicals of reactions R155, R431, R45, R199, R510, R526, R1112, and R1134 follows the order DME/CH_4

$> \text{DME}/\text{C}_4\text{H}_{10} > \text{DME}/\text{C}_2\text{H}_6 > \text{DME}/\text{C}_3\text{H}_8$ and the time corresponding to the production rate peak increases in the order $\text{DME}/\text{CH}_4 < \text{DME}/\text{C}_4\text{H}_{10} < \text{DME}/\text{C}_2\text{H}_6 < \text{DME}/\text{C}_3\text{H}_8$. Thus, the ignition delay increases in the order $\text{DME}/\text{CH}_4 < \text{DME}/\text{C}_4\text{H}_{10} < \text{DME}/\text{C}_2\text{H}_6 < \text{DME}/\text{C}_3\text{H}_8$. As shown in Figure 9c, at $T_c = 1500$ K, the OH radicals production rate of reaction R5 and R98 follows the order $\text{DME}/\text{C}_2\text{H}_6 > \text{DME}/\text{C}_4\text{H}_{10} > \text{DME}/\text{C}_3\text{H}_8 > \text{DME}/\text{CH}_4$ and the time corresponding to the production rate peak increases in the order $\text{DME}/\text{C}_2\text{H}_6 < \text{DME}/\text{C}_4\text{H}_{10} < \text{DME}/\text{C}_3\text{H}_8 < \text{DME}/\text{CH}_4$. As a result, the ignition delay increases in the order $\text{DME}/\text{C}_2\text{H}_6 < \text{DME}/\text{C}_4\text{H}_{10} < \text{DME}/\text{C}_3\text{H}_8 < \text{DME}/\text{CH}_4$.

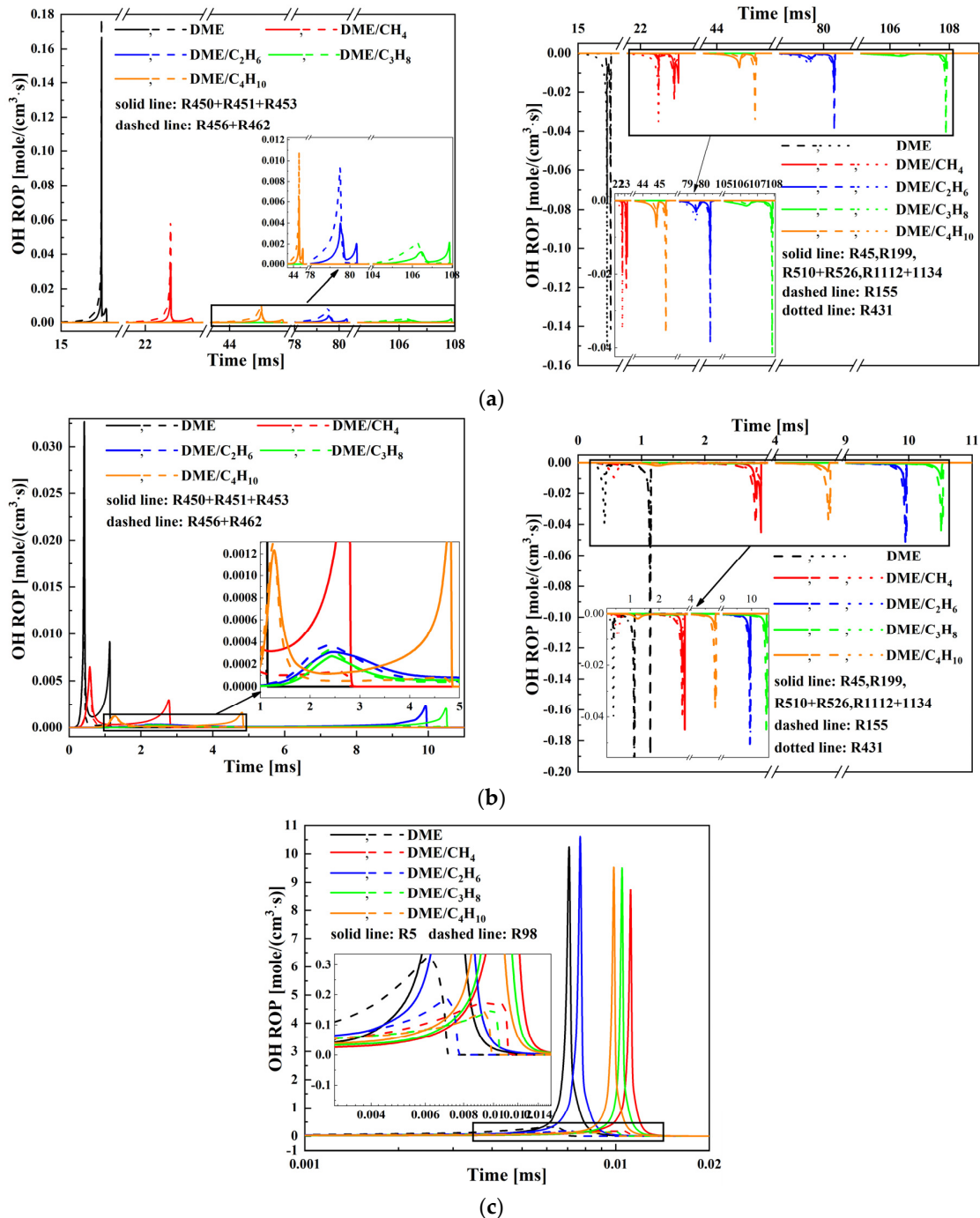


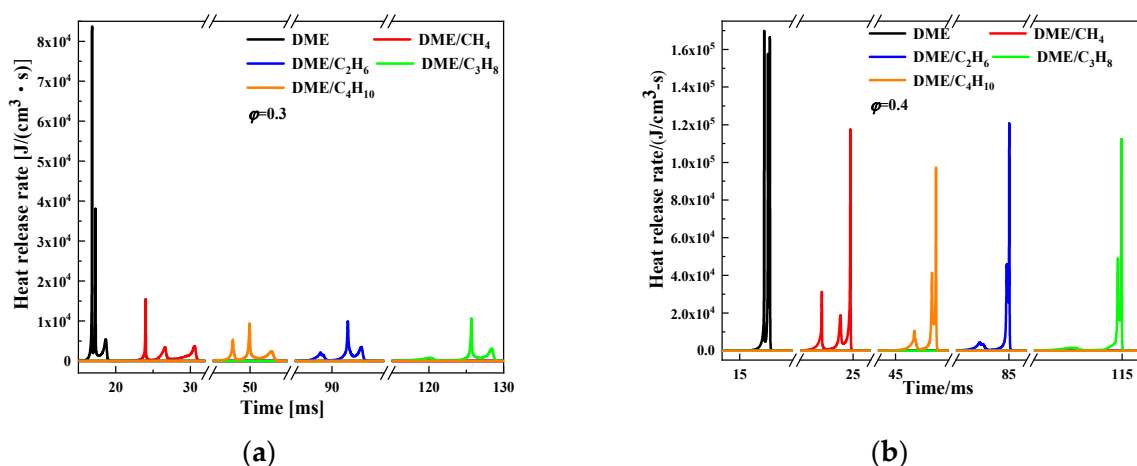
Figure 9. Production rate of OH radicals of the important elementary reactions for various compressed temperatures at $P_c = 20$ bar and $\phi = 0.5$: (a) $T_c = 650$ K; (b) $T_c = 800$ K; and (c) $T_c = 1500$ K.

Table 2. Important elementary reactions involving OH radicals.

| Reaction Number | Reaction Equation |
|-----------------|---|
| R5 | $O_2 + H \rightleftharpoons O + OH$ |
| R45 | $CH_4 + OH \rightleftharpoons CH_3 + H_2O$ |
| R98 | $CH_3 + HO_2 \rightleftharpoons CH_3O + OH$ |
| R155 | $CH_2O + OH \rightleftharpoons HCO + H_2O$ |
| R199 | $C_2H_6 + OH \rightleftharpoons C_2H_5 + H_2O$ |
| R431 | $CH_3OCH_3 + OH \rightleftharpoons CH_3OCH_2 + H_2O$ |
| R450 | $CH_3OCH_2 + O_2 \rightleftharpoons 2CH_2O + OH$ |
| R451 | $CH_3OCH_2O_2 \rightleftharpoons 2CH_2O + OH$ |
| R453 | $CH_2OCH_2O_2H \rightleftharpoons 2CH_2O + OH$ |
| R456 | $O_2CH_2OCH_2O_2H \rightleftharpoons HO_2CH_2OCHO + OH$ |
| R462 | $HO_2CH_2OCHO \rightleftharpoons OCH_2OCHO + OH$ |
| R510 | $C_3H_8 + OH \rightleftharpoons NC_3H_7 + H_2O$ |
| R526 | $C_3H_8 + OH \rightleftharpoons IC_3H_7 + H_2O$ |
| R1112 | $C_4H_{10} + OH \rightleftharpoons PC_4H_9 + H_2O$ |
| R1134 | $C_4H_{10} + OH \rightleftharpoons SC_4H_9 + H_2O$ |

3.2. Multi-Stage Ignition Characteristic of DME/C1-C4 Alkane Mixtures

Figures 10 and 11 present the HRR and pressure of DME/C1-C4 alkane (50%/50%) mixtures as a function of time at different equivalence ratios of $\varphi = 0.3, 0.4,$ and $0.5,$ respectively. DME/C1-C4 alkane mixtures display a three-stage heat release phenomenon, which are low temperature reaction, high temperature first stage reaction, and high temperature second stage reaction. The C1-C4 alkane addition on DME ignition will decrease the pressure and heat release peak and delay the time corresponding to the pressure and heat release peak. At the same equivalence ratio, the difference of the pressure peak of the mixtures is small, but the difference of the time corresponding to the pressure and heat release peak is large. The time corresponding to the heat release and pressure peak increases in the order $DME/CH_4 < DME/C_4H_{10} < DME/C_2H_6 < DME/C_3H_8$. The maximum value of the heat release peak of the mixtures appears in the high temperature second stage reaction at the equivalence ratios of 0.3 and 0.4, whereas the maximum value appears in the high temperature first stage reaction at the equivalence ratio of 0.3.

**Figure 10.** Cont.

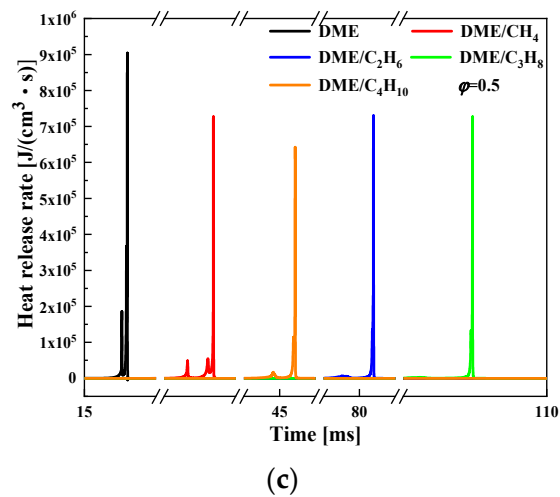


Figure 10. Comparison of heat release rate of DME/C1-C4 alkane mixtures for various equivalence ratios at $T_c = 650$ K and $P_c = 20$ bar: (a) $\phi = 0.3$; (b) $\phi = 0.4$; and (c) $\phi = 0.5$.

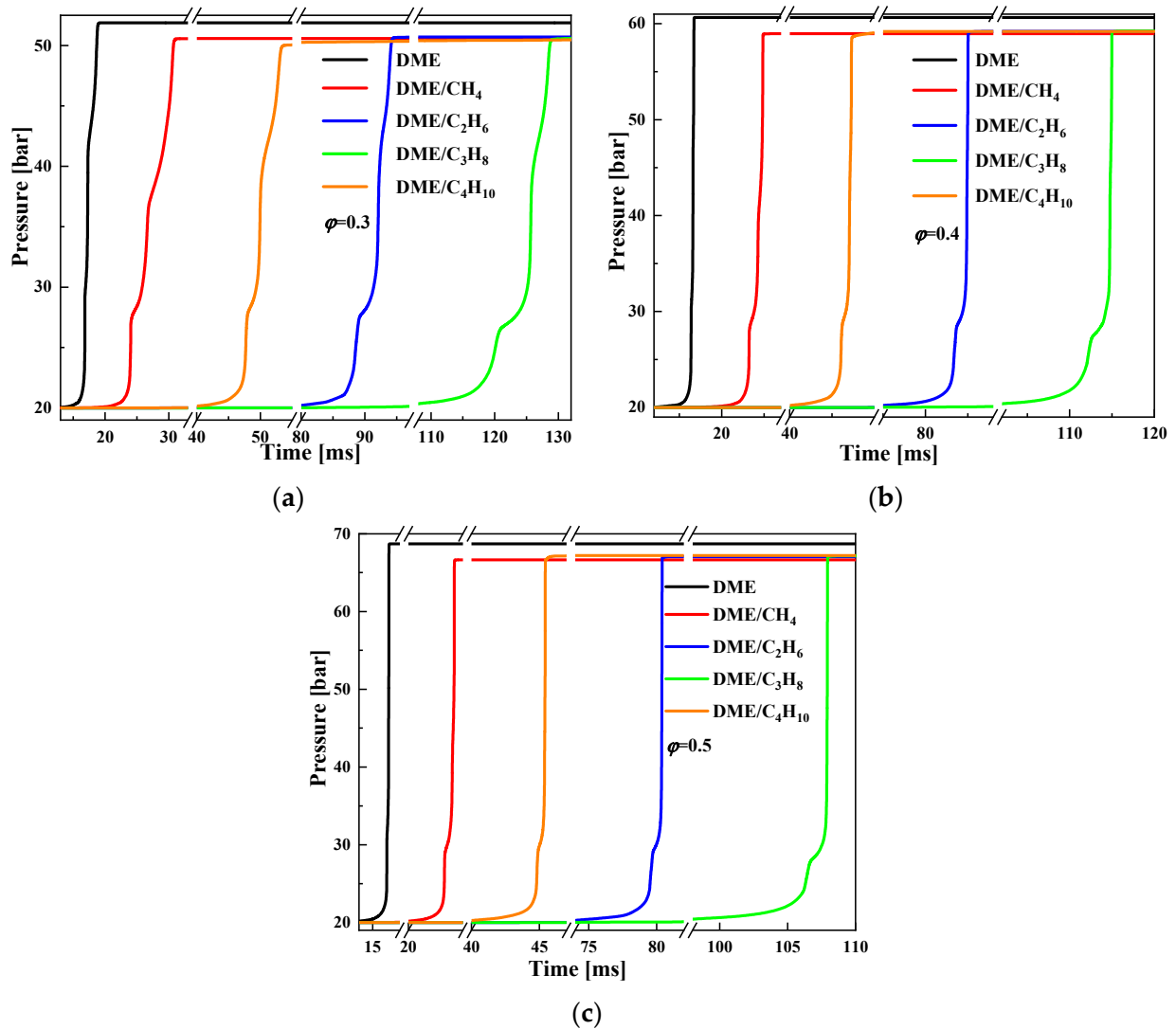


Figure 11. Comparison of pressure of DME/C1-C4 alkane mixtures for various equivalence ratios at $T_c = 650$ K and $P_c = 20$ bar: (a) $\phi = 0.3$; (b) $\phi = 0.4$; and (c) $\phi = 0.5$.

In order to further illustrate the three-stage ignition and heat release characteristic of DME/C1-C4 alkane mixtures at low-temperature and lean-burn conditions, the HRR of the important elementary reactions is plotted as a function of temperature at $\varphi = 0.4$ in Figure 12. The important elementary reactions which contribute to the HRR are listed in Table 3. As presented in Figure 12 and Table 3, the heat produced by reactions R2, R3, R4, R5, and R6 dominate the high temperature first stage reaction, whereas the heat produced by reactions R2, R7, and R8 dominate the high temperature second stage reaction.

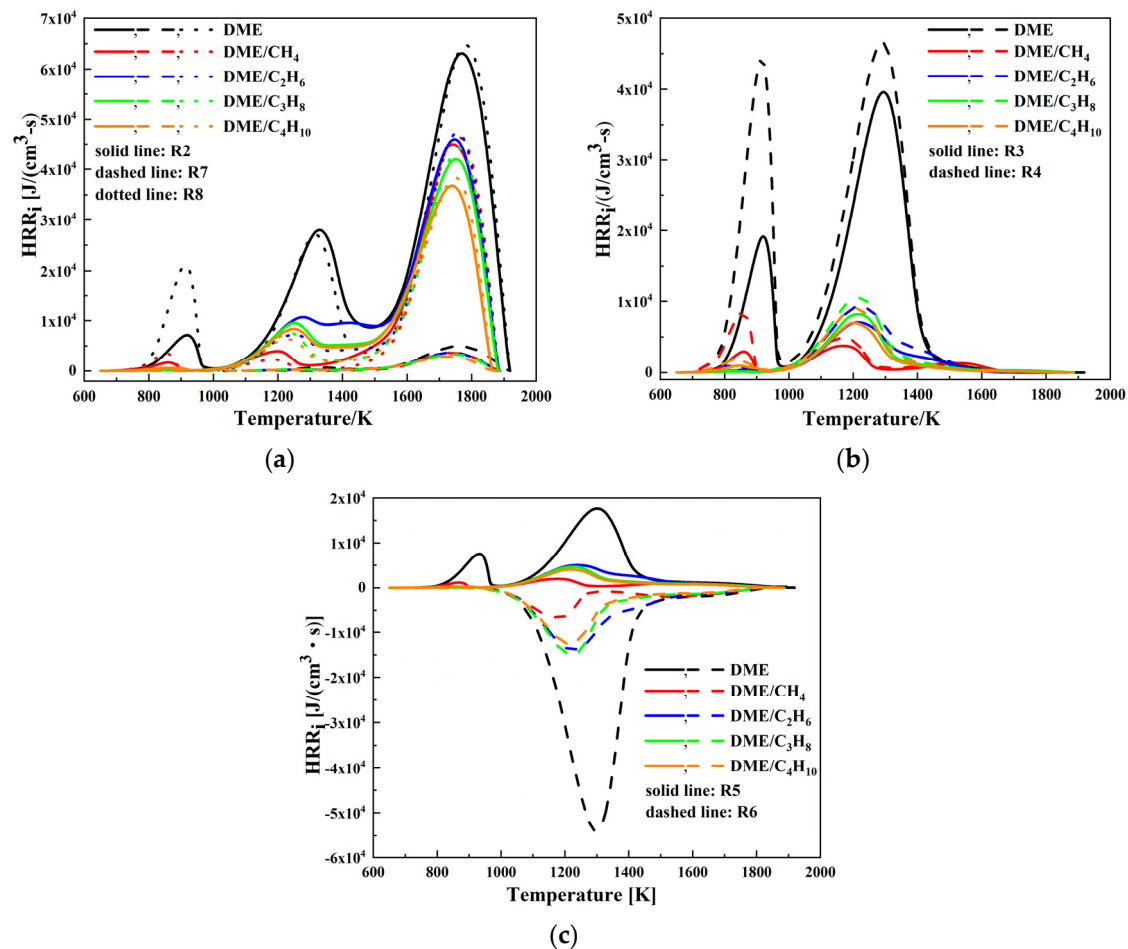


Figure 12. Heat release rate for various important elementary reactions at $T_c = 650$ K, $P_c = 20$ bar, and $\varphi = 0.4$: (a) R2, R7, R8; (b) R3, R4; and (c) R5, R6.

Table 3. Important elementary reactions contributing to the heat release rate.

| Reaction Number | Reaction Equation |
|-----------------|---|
| R2 | $\text{H} + \text{O}_2 + \text{M} \rightleftharpoons \text{HO}_2 + \text{M}$ |
| R3 | $\text{HCHO} + \text{OH} \rightleftharpoons \text{HCO} + \text{H}_2\text{O}$ |
| R4 | $\text{HCO} + \text{O}_2 \rightleftharpoons \text{CO} + \text{HO}_2$ |
| R5 | $\text{HO}_2 + \text{HO}_2 \rightleftharpoons \text{H}_2\text{O}_2 + \text{O}_2$ |
| R6 | $\text{H}_2\text{O}_2 + \text{M} \rightleftharpoons \text{OH} + \text{OH} + \text{M}$ |
| R7 | $\text{CO} + \text{OH} \rightleftharpoons \text{CO}_2 + \text{H}$ |
| R8 | $\text{HO}_2 + \text{OH} \rightleftharpoons \text{H}_2\text{O} + \text{O}_2$ |

The HO_2 radicals produced by reaction R2 feed reaction R5 and form the H_2O_2 radicals; thereby, the H_2O_2 radicals accumulated by reaction R5 feed reaction R6 and produce the OH radicals. Meanwhile, the OH radicals are used to consume HCHO through reaction R3 and produce HCO radicals. The HCO radicals are consumed by reaction R4 and form CO.

It can be concluded that the heat release during the high temperature first stage reaction is mainly caused by CO produced by the consumption of HCHO. The HRR of reactions R3, R4, R5, and R6 decreases in the order DME/C₃H₈ > DME/C₂H₆ > DME/C₄H₁₀ > DME/CH₄. Therefore, the heat release peak of the high temperature first stage reaction decreases in the order DME/C₃H₈ > DME/C₂H₆ > DME/C₄H₁₀ > DME/CH₄. In addition, the HO₂ radicals produced by reaction R2 feed reaction R8 and produce H₂O, and the OH radicals are consumed by reaction R7 and form CO₂. It can be concluded that the heat release during the high temperature first stage reaction is mainly caused by CO₂ and H₂O produced by the consumption of CO and HO₂. The HRR of reactions R2, R7, and R8 decreases in the order DME/C₂H₆ > DME/CH₄ > DME/C₃H₈ > DME/C₄H₁₀. As a consequence, the heat release peak of the high temperature second stage reaction decreases in the order DME/C₂H₆ > DME/CH₄ > DME/C₃H₈ > DME/C₄H₁₀.

4. Conclusions

In this study, the CHEMKIN-PRO software is used to calculate the ignition delay and multi-stage ignition process of DME/C1-C4 alkane mixtures under engine relevant low-temperature and high-pressure conditions. The main conclusions are as follows:

(1) The DME/C1-C4 alkane mixtures exhibit a typical NTC characteristic over the temperature range of 750–900 K as the temperature increases. In the NTC region, the ignition delay decreases in the order DME/C₃H₈ > DME/C₂H₆ > DME/C₄H₁₀ > DME/CH₄. The initial temperature of DME/CH₄ mixtures of the NTC region is the highest, and DME/C₄H₁₀ mixtures have the most obvious NTC phenomenon. With the increase of pressure and equivalence ratio, the ignition delay presents a nonlinear decreasing trend and the effect becomes significant at a lower pressure and equivalence ratio.

(2) At low temperature and low equivalence ratio conditions, DME/C1-C4 alkane mixtures show a distinct three-stage heat release characteristic. The time corresponding to the pressure and HRR peak increases in the order DME/CH₄ < DME/C₄H₁₀ < DME/C₂H₆ < DME/C₃H₈. At the equivalence ratio of 0.4, the heat release peak of the high temperature first stage reaction decreases in the order DME/C₃H₈ > DME/C₂H₆ > DME/C₄H₁₀ > DME/CH₄ and the heat release peak of the high temperature second stage reaction decreases in the order DME/C₂H₆ > DME/CH₄ > DME/C₃H₈ > DME/C₄H₁₀.

(3) Kinetic analysis indicates that methane and ethane show an obvious single-stage ignition characteristic, whereas DME, propane, and n-butane exhibit a typical two-stage ignition characteristic. The heat and free radicals produced during the first-stage ignition determine the second-stage ignition when the mixtures display two-stage ignition behavior. Small molecular alkane competes with the OH radicals generated in the oxidation process of DME, which inhibits the oxidation of DME and promotes the oxidation of small molecular alkane. The concentration of active radicals and the OH radical production rate of elementary reaction for DME/CH₄ mixtures are the highest and DME/C₃H₈ mixtures are the lowest. At the equivalence ratio of 0.4, the heat produced by reactions R2, R3, R4, R5, and R6 dominate the high temperature first stage reaction, whereas the heat produced by reactions R2, R7, and R8 dominate the high temperature second stage reaction. In addition, the HRR of reactions R3, R4, R5, and R6 decreases in the order DME/C₃H₈ > DME/C₂H₆ > DME/C₄H₁₀ > DME/CH₄ and the HRR of reactions R2, R7, and R8 decreases in the order DME/C₂H₆ > DME/CH₄ > DME/C₃H₈ > DME/C₄H₁₀.

Author Contributions: Conceptualization, K.N. and B.Y.; methodology, K.N.; software, Y.X.; validation, Z.S.; formal analysis, K.N.; investigation, H.Z.; resources, Y.W.; data curation, Y.W.; writing—original draft preparation, K.N.; writing—review and editing, Y.X.; visualization, B.Y.; supervision, H.Z.; project administration, Z.S.; funding acquisition, H.Z. All authors have read and agreed to the published version of the manuscript.

Funding: This work was sponsored by the Beijing Natural Science Foundation (grant No. 3222024) and supported by the State Key Laboratory of Engines, Tianjin University (grant No. K2020-08).

Institutional Review Board Statement: Not applicable.

Informed Consent Statement: Not applicable.

Data Availability Statement: Not applicable.

Acknowledgments: The authors would like to thank the reviewers for their valuable comments on this research.

Conflicts of Interest: The authors declare no conflict of interest.

References

1. Zhu, D.C.; Zhao, R.N.; Wu, H.; Shi, Z.C.; Li, X.R. Experimental study on combustion and emission characteristics of diesel engine with high supercharged condition. *Chemosphere* **2022**, *304*, 135336. [[CrossRef](#)]
2. Arcoumains, C.; Bae, C.; Crookes, R.; Kinoshita, E. The potential of dimethyl ether (DME) as an alternative fuel for compression-ignition engines: A review. *Fuel* **2008**, *87*, 1014–1030. [[CrossRef](#)]
3. Park, S.H.; Lee, C.S. Applicability of dimethyl ether (DME) in a compression ignition engine as an alternative fuel. *Energy Conv. Manag.* **2014**, *86*, 848–863. [[CrossRef](#)]
4. Yao, M.F.; Zheng, Z.L.; Liu, H.F. Progress and recent trends in homogeneous charge compression ignition (HCCI) engines. *Prog. Energy Combust. Sci.* **2009**, *35*, 398–437. [[CrossRef](#)]
5. Hasan, M.M.; Rahman, M.M. Homogeneous charge compression ignition combustion: Advantages over compression ignition combustion, challenges and solutions. *Renew. Sustain. Energy Rev.* **2016**, *57*, 282–291. [[CrossRef](#)]
6. Bendu, H.; Murugan, S. Homogeneous charge compression ignition (HCCI) combustion: Mixture preparation and control strategies in diesel engines. *Renew. Sustain. Energy Rev.* **2014**, *38*, 732–746. [[CrossRef](#)]
7. Jung, D.; Kwon, O.; Lim, O.T. Comparison of DME HCCI operating ranges for the thermal stratification and fuel stratification based on a multi-zone model. *J. Mech. Sci. Technol.* **2011**, *25*, 1383–1390. [[CrossRef](#)]
8. Lu, X.C.; Han, D.; Huang, Z. Fuel design and management for the control of advanced compression-ignition combustion modes. *Prog. Energy Combust. Sci.* **2011**, *37*, 741–783. [[CrossRef](#)]
9. Duan, X.B.; Lai, M.C.; Jansons, M.; Guo, G.M.; Liu, J.P. A review of controlling strategies of the ignition timing and combustion phase in homogeneous charge compression ignition (HCCI) engine. *Fuel* **2021**, *285*, 119142. [[CrossRef](#)]
10. Shi, Z.; Zhang, H.; Lu, H.; Liu, H.; Yunsheng, A.; Meng, F. Autoignition of DME/H₂ mixtures in a rapid compression machine under low-to-medium temperature ranges. *Fuel* **2017**, *194*, 50–62. [[CrossRef](#)]
11. Mittal, G.; Chaos, M.; Sung, C.J.; Dryer, F.L. Dimethyl ether autoignition in a rapid compression machine: Experiments and chemical kinetic modeling. *Fuel Process. Technol.* **2008**, *89*, 1244–1254. [[CrossRef](#)]
12. Cook, R.D.; Davidson, D.F.; Hanson, R.K. Shock tube measurements of ignition delay times and OH time-histories in dimethyl ether oxidation. *Proc. Combust. Inst.* **2009**, *32*, 189–196. [[CrossRef](#)]
13. Li, Z.H.; Wang, W.J.; Huang, Z.; Oehlschlaeger, M.A. Dimethyl ether autoignition at Engine-Relevant conditions. *Energy Fuels* **2013**, *27*, 2811–2817. [[CrossRef](#)]
14. Pan, L.; Hu, E.J.; Tian, Z.M.; Yang, F.Y.; Huang, Z.H. Experimental and kinetic study on ignition delay times of dimethyl ether at high temperatures. *Energy Fuels* **2015**, *29*, 3495–3506. [[CrossRef](#)]
15. Schonborn, A.; Sayad, P.; Konnov, A.A.; Klingmann, J. Autoignition of dimethyl ether and air in an optical flow-reactor. *Energy Fuels* **2014**, *28*, 4130–4138. [[CrossRef](#)]
16. Fischer, S.L.; Dryer, F.L.; Curran, H.J. The reaction kinetics of dimethyl ether. I: High-temperature pyrolysis and oxidation in flow reactors. *Int. J. Chem. Kinet.* **2000**, *32*, 713–740. [[CrossRef](#)]
17. Curran, H.J.; Fischer, S.L.; Dryer, F.L. The reaction kinetics of dimethyl ether. II: Low-temperature oxidation in flow reactors. *Int. J. Chem. Kinet.* **2000**, *32*, 741–759. [[CrossRef](#)]
18. Dagaut, P.; Daly, C.; Simmie, J.M.; Cathonnet, M. The oxidation and ignition of dimethyl ether from low to high temperature (500–1600 K): Experiments and kinetic modeling. *Symp. Int. Combust.* **1998**, *27*, 361–369. [[CrossRef](#)]
19. Liu, H.; Zhang, H.G.; Shi, Z.C.; Lu, H.T.; Zhao, G.Y.; Yao, B.F. Performance characterization and auto-ignition performance of a rapid compression machine. *Energies* **2014**, *7*, 6083–6104. [[CrossRef](#)]
20. Shi, Z.C.; Zhang, H.G.; Liu, H.; Lu, H.T.; Lia, J.Z.; Gao, X. Effects of buffer gas composition on autoignition of dimethyl ether. *Energies* **2015**, *8*, 10198–10218. [[CrossRef](#)]
21. Burke, U.; Somers, K.P.; O’Toole, P.; Zinner, C.M.; Marquet, N.; Bourque, G.; Petersen, E.L.; Metcalfe, W.K.; Serinyel, Z.; Curran, H.J. An ignition delay and kinetic modeling study of methane, dimethyl ether, and their mixtures at high pressures. *Combust. Flame* **2015**, *162*, 315–330. [[CrossRef](#)]
22. Tang, C.L.; Wei, L.J.; Zhang, J.X.; Man, X.J.; Huang, Z.H. Shock tube measurements and kinetic investigation on the ignition delay times of methane/dimethyl ether mixtures. *Energy Fuels* **2012**, *26*, 6720–6728. [[CrossRef](#)]
23. Shi, Z.C.; Wu, H.; Zhang, H.G.; Wang, Z.M.; Lee, C.F.; Xu, Y.H. Autoignition of DME/C₂H₆ mixtures under high-pressure and low-temperature conditions. *Combust. Sci. Technol.* **2018**, *191*, 1201–1218. [[CrossRef](#)]
24. Zhang, J.X.; Hu, E.J.; Pan, L.; Zhang, Z.H.; Huang, Z.H. Shock-tube measurements of ignition delay times for the ethane/dimethyl ether blends. *Energy Fuels* **2013**, *27*, 6247–6254. [[CrossRef](#)]

25. Lu, L.X.; Zou, C.; Xia, W.X.; Lin, Q.J.; Shi, H.Y. Experimental and numerical study on the ignition delay times of dimethyl ether/ethane/oxygen/carbon dioxide mixtures. *Fuel* **2020**, *280*, 118675. [[CrossRef](#)]
26. Dames, E.E.; Rosen, A.S.; Weber, B.W.; Gao, C.W.; Sung, C.J.; Green, W.H. A detailed combined experimental and theoretical study on dimethyl ether/propane blended oxidation. *Combust. Flame* **2016**, *168*, 310–330. [[CrossRef](#)]
27. Hu, E.J.; Zhang, Z.H.; Pan, L.; Zhang, J.X.; Huang, Z.H. Experimental and modeling study on ignition delay times of dimethyl ether/propane/oxygen/argon mixtures at 20 bar. *Energy Fuels* **2013**, *27*, 4007–4013. [[CrossRef](#)]
28. Wu, H.; Shi, Z.C.; Lee, C.F.; Zhang, H.G.; Xu, Y.H. Experimental and kinetic study on ignition of DME/n-butane mixtures under high pressures on a rapid compression machine. *Fuel* **2018**, *225*, 35–46. [[CrossRef](#)]
29. Jiang, X.; Zhang, Y.J.; Man, X.J.; Pan, L.; Huang, Z.H. Shock tube measurements and kinetic study on ignition delay times of lean DME/n-butane blends at elevated pressures. *Energy Fuels* **2013**, *27*, 6238–6246. [[CrossRef](#)]
30. Jiang, X.; Tian, Z.M.; Zhang, Y.J.; Huang, Z.H. Shock tube measurement and simulation of DME/n-butane/air mixtures: Effect of blending in the NTC region. *Fuel* **2017**, *203*, 316–329. [[CrossRef](#)]
31. Hu, E.J.; Huang, Z.H.; Jiang, X.; Zhang, J.X. *Study on Ignition Delay Times of DME and n-Butane Blends*; SAE Technical Paper; SAE International: Warrendale, PA, USA, 2013. [[CrossRef](#)]
32. Hu, E.J.; Jiang, X.; Huang, Z.H.; Zhang, J.X.; Zhang, Z.H.; Man, X.J. Experimental and kinetic studies on ignition delay times of dimethyl ether/n-butane/O₂/Ar mixtures. *Energy Fuels* **2013**, *27*, 530–536. [[CrossRef](#)]
33. Jiang, X.; Zhang, Y.J.; Man, X.J.; Pan, L.; Huang, Z.H. Experimental and modeling study on ignition delay times of dimethyl ether/n-butane blends at a pressure of 2.0 MPa. *Energy Fuels* **2014**, *28*, 2189–2198. [[CrossRef](#)]
34. Jiang, X.; Zhang, Y.J.; Pan, L.; Man, X.J.; Huang, Z.H. *Experimental and Modeling Study on Auto-Ignition of DME/n-Butane Blends under Engine Relevant Pressure*; SAE Technical Paper; SAE International: Warrendale, PA, USA, 2014. [[CrossRef](#)]
35. Oshibe, H.; Nakamura, H.; Tezuka, T.; Hasegawa, S.; Maruta, K. Stabilized three-stage oxidation of DME/air mixture in a micro flow reactor with a controlled temperature profile. *Combust. Flame* **2010**, *157*, 1572–1580. [[CrossRef](#)]
36. Lim, O.T. Numerical analysis of the effect of inhomogeneous pre-mixture on the pressure rise rate in an HCCI engine using multi-zone chemical kinetics. *Int. J. Automot. Technol.* **2014**, *15*, 535–541. [[CrossRef](#)]
37. Iijima, A.; Tsutsumi, Y.; Yoshida, K.; Shoji, H. *Spectroscopic Study of Two-Stage High Temperature Heat Release Behavior in a Supercharged HCCI Engine Using Blended Fuels*; SAE Technical Paper; SAE International: Warrendale, PA, USA, 2011. [[CrossRef](#)]
38. Shimizu, R.; Iijima, A.; Yoshida, K.; Shoji, H. *Analysis of Supercharged HCCI Combustion Using a Blended Fuel*; SAE Technical Paper; SAE International: Warrendale, PA, USA, 2011. [[CrossRef](#)]
39. Komatsu, K.; Asanuma, M.; Iijima, A.; Yoshida, K.; Shoji, H. *A Study of an HCCI Engine Operating on a Blended Fuel of DME and Methane*; SAE Technical Paper; SAE International: Warrendale, PA, USA, 2011. [[CrossRef](#)]
40. Zhou, C.W.; Li, Y.; Burke, U.; Banyon, C.; Somers, K.P.; Ding, S.T.; Khan, S.; Hargis, J.W.; Sikes, T.; Mathieu, O. An experimental and chemical kinetic modeling study of 1,3-butadiene combustion: Ignition delay time and laminar flame speed measurements. *Combust. Flame* **2018**, *197*, 423–438. [[CrossRef](#)]